Electric Field Effects of Photogenerated Ion Pairs on Nearby Molecules: A Model for the Carotenoid Band Shift in Photosynthesis

David Gosztola,† Hiroko Yamada,† and Michael R. Wasielewski*,†,‡

Contribution from the Chemistry Division, Argonne National Laboratory, Argonne, Illinois 60439-4831, and Department of Chemistry, Northwestern University, Evanston, Illinois 60208-3113

Received May 2, 1994[⊗]

Abstract: Photoinduced charge separation within a zinc porphyrin electron donor−pyromellitimide electron acceptor pair possessing an 8.4 Å center-to-center distance and a linear orientation is shown to induce large electrochromic effects on the ground state absorption spectrum of a nearby carotenoid molecule. The orientation of the C−C backbone of the carotenoid is restricted relative to the direction of the electric field produced by the photogenerated ion pair. This is accomplished by covalently linking the electron donor−acceptor pair to the carotenoid with a calix[4]arene bridge. The bridge maintains its cone conformation resulting in an average dihedral angle of 35° between the donor−acceptor axis and the C−C backbone of the carotenoid. Using picosecond transient absorption spectroscopy, a 15 nm electrochromic red shift in the ground state absorption spectrum of the carotenoid was readily observed during the 3.7 ns lifetime of the photogenerated ion pair. The magnitude of this shift depends on the dielectric constant of the surrounding solvent. The data is used to calculate an electric field strength of about 5.5 MV/cm at the carotenoid in toluene. The magnitude of the electric field produced by the ion pair at the carotenoid is larger than the highest fields that can be applied externally. This approach can be used to study the influence of electric fields produced by ion pairs on the photophysics and photochemistry of nearby molecules.

Introduction

Covalently-linked arrays of electron donors and acceptors are often used to study photoinitiated electron transfer reactions that mimic natural photosynthesis.[1,2] Charge separation within these arrays can produce ion pairs that live as long as milliseconds before recombining. In addition, the medium surrounding these donors and acceptors is known to have a significant influence on the rates and energetics of these reactions.[3] In turn, the dipolar ion pair products of these reactions generate large electric fields that can significantly perturb the electronic structures of nearby molecules. These perturbations may result in changes in the photophysics of adjacent chromophores and/or the kinetics of electron transfer in nearby donor−acceptor pairs. Studies of electrochromic spectral shifts of carotenoids[4,5] and chlorophylls[6,7] within membrane-bound proteins conclude that electric fields on the order of 10^6 V/cm are generated as a consequence of photosynthetic charge separation across the membrane. Application of an electric field to oriented samples of bacterial reaction center proteins results in significant changes in the rate constants for electron transfer reactions involving the cofactors within the protein.[8]

Measurements of electric field effects on chromophores alone often utilize a thin film capacitor consisting of a pair of conductive, optically transparent electrodes between which is placed a thin film of a dielectric medium containing a solid solution of the chromophore.[9] The chromophores are randomly oriented relative to the electric field direction. Application of an external voltage to the plates can generate electric fields on the order of 10^6 V/cm. The intervening dielectric medium alters the applied field so that the actual field at the sample differs from the applied field. Accurate assessments of this effect, the so-called local field correction, are difficult.

In this paper we describe a different strategy to study the effects of the electric field produced by a photogenerated ion pair on nearby molecules. This approach uses a photochemical electron donor−acceptor pair as the electric field generator. This donor−acceptor pair possesses a restricted donor−acceptor distance and geometry, well-characterized transient ion pair spectra, and a quantum yield of charge separation near unity. Thus, the electric field can be turned on photochemically. This donor−acceptor field generator is positioned at a restricted distance and geometry relative to a nearby probe molecule by covalent attachment of these two molecules to a hydrocarbon spacer. The ideal probe molecule should possess photophysical properties that are sensitive to both the strength and orientation of the electric field. In principal, the probe may also be another donor−acceptor molecule. The presence of the electric field generated by the initial ion pair formation can influence the free energy of charge separation in the second donor−acceptor pair in a manner similar to the effects of external fields on electron transfer rates in proteins mentioned above.

Our initial efforts in this direction have produced molecule **1** in which the electric field effect of a photogenerated ion pair

† Argonne National Laboratory.
‡ Northwestern University.
⊗ Abstract published in *Advance ACS Abstracts,* February 1, 1995.

(1) Wasielewski, M. R. *Chem. Rev.* **1992**, *92*, 435.
(2) Gust, D.; Moore, T. A.; Moore, A. L. *Acc. Chem. Res.* **1993**, *26*, 198.
(3) Closs, G. L.; Miller, J. R. *Science* **1988**, *240*, 440.
(4) Junge, W.; Witt, H. T. *Z. Naturforsch. B* **1968**, *23*, 244.
(5) Crofts, A. R.; Prince, R. C.; Holmes, N. G.; Crowther, D. In *Proceedings of the Third International Congress on Photosynthesis*; Avron, M., Ed.; Elsevier Scientific: Amsterdam, 1974; p 1131.
(6) Emrich, H. M.; Junge, W.; Witt, H. T. *Z. Naturforsch. B* **1969**, *24*, 1144.
(7) Amesz, J.; Visser, J. W. M. *Biochim. Biophys. Acta* **1971**, *234*, 62.
(8) (a) Alegria, G.; Dutton, P. L. *Biochim. Biophys. Acta* **1991**, *1057*, 239. (b) Alegria, G.; Dutton, P. L. *Biochim. Biophys. Acta* **1991**, *1057*, 258.
(9) Boxer, S. G. In *The Photosynthetic Reaction Center*; Deisenhofer, J., Norris, J. R., Eds.; Academic Press: San Diego, 1993; Vol. 2, p 179.

0002-7863/95/1517-2041$09.00/0

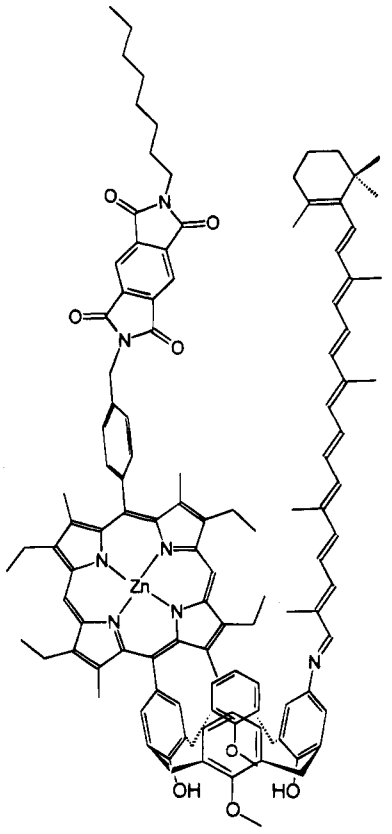

1

on an adjacent chromophore can be probed at close distances with a minimum number of solvent molecules between the field generator and the probe. An intense electric field is generated by the ion pair product that results from oxidation of the lowest excited singlet state of a Zn porphyrin, ZP, by a covalently-attached pyromellitimide acceptor, PI. The ZP^+-PI^- ion pair maintains an 8.4 Å center-to-center distance[10] that is restricted by the covalent attachment. The ZP^+-PI^- ion pair, in turn, is attached to a calix[4]arene spacer that exists in its cone conformation.[11] Attachment of a carotenoid probe molecule to the calix[4]arene about 8 Å away from ZP^+-PI^- restricts the overall average orientation of the electric field generator relative to that of the probe molecule in **1**. Although the phenolic residues of the calix[4]arene are not completely rigid relative to one another, hydrogen bonding of the OH groups at the lower rim of the calix[4]arene to the adjacent OCH_3 groups enforces the cone configuration. An advantage of this approach is that the average orientation of the electric field produced by ZP^+-PI^- relative to the orientation of the probe molecule is maintained by the molecular structure of the calix[4]arene spacer, even though the entire supramolecular assembly rotates in liquid solution. Thus, measurements made in solution allow us to probe the directional nature of the electric field effect on the probe molecule.

Results

Synthesis. The calix[4]arene molecule was chosen as the spacer to hold the donor–acceptor pair in a restricted orientation relative to the carotenoid probe molecule. It is well-known that two of the four phenolic hydroxyl groups that are opposite one another in the calix[4]arene can be selectively methylated.[12] The hydrogen bonding that occurs between the remaining phenolic OH groups and the methoxy groups of the adjacent anisoles results in a strong preference for the so-called cone conformation of the calix[4]arene in solution.[11] This conformation results in a characteristic AB quartet centered at about $\delta = 3.8$ ppm in the proton NMR spectrum of 26,28-dihydroxy-25,27-dimethoxycalix[4]arene, **2**. The greater reactivity of the phenols

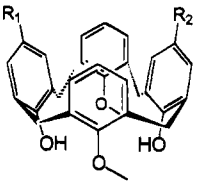

2: $R_1 = R_2 = H$
3: $R_1 = CHO$; $R_2 = H$
4: $R_1 = CHO$; $R_2 = NO_2$
9: $R_1 = NO_2$; $R_2 = H$
10: $R_1 = NH_2$; $R_2 = H$

toward electrophilic substitution in **2** results in selective functionalization of the phenols at their position *para* to the hydroxyl group. On average, these *para* substituents will point away from the oxygen atoms at the lower rim of the calix[4]-arene. Further functionalization of the oxygen atoms at the lower rim provides a convenient method of altering the conformation of the phenols relative to one another.[13]

Compound **2** was readily formylated using $Cl_2CHOCH_3/TiCl_4$ in CH_2Cl_2 to give an 82% yield of the monoformyl derivative.[12] The resulting 5-formyl derivative, **3**, was nitrated[12] using HNO_3 in acetic anhydride/CH_2Cl_2 to give the 5-formyl-17-nitrocalix-[4]arene **4** in 62% yield. Derivative **4** is a basic building block from which a variety of molecules can be prepared. Preparation of the aldehyde bearing the pyromellitimide electron acceptor, *N*-((4-formylphenyl)methyl)-*N'*-octyl-1,2:4,5-benzenebis(dicarboximide), **5**, has been described previously.[14] One equivalent

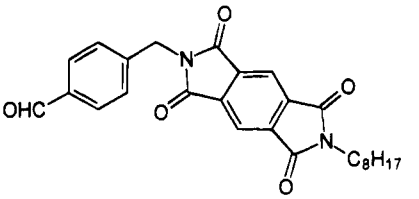

5

each of aldehydes **4** and **5** were reacted with 2 equiv of 3,3'-dimethyl-4,4'-diethyldipyrrylmethane, **6**,[15] in 1/1 CH_2Cl_2/CH_3-

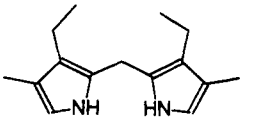

6

CN using CCl_3CO_2H as the acid catalyst, followed by *in situ*

(10) Molecular structure parameters were determined from an MM2 energy-minimized structure using Hyperchem software (Hypercube: Waterloo, Ontario, Canada).
(11) Gutsche, C. D. *Calixarenes*; Royal Society of Chemistry: Cambridge, 1989; Chapter 4.
(12) van Loon, J.-D.; Arduini, A.; Coppi, L.; Verboom, W.; Pochini, A.; Ungaro, R.; Harkema, S.; Reinhoudt, D. N. *J. Org. Chem.* **1990**, *55*, 5639.
(13) Shinkai, S. *Tetrahedron* **1993**, *49*, 8933.
(14) Osuka, A.; Zhang, R.-P.; Maruyama, K.; Ohno, T.; Nozaki, K. *Bull. Chem. Soc. Jpn.* **1993**, *66*, 3773.
(15) Bullock, E.; Johnson, A. W.; Markham, E.; Shaw, K. B. *J. Chem. Soc.* **1958**, 1430.

oxidation of the porphyrinogen with chloranil[16] to give a 22% yield of a porphyrin–pyromellitimide unit substituted at the 5-position of the 17-nitrocalix[4]arene. Zinc was inserted quantitatively into the porphyrin by stirring the free base with methanolic $Zn(OAc)_2$ in $CHCl_3$ to yield **7**. The nitro group of

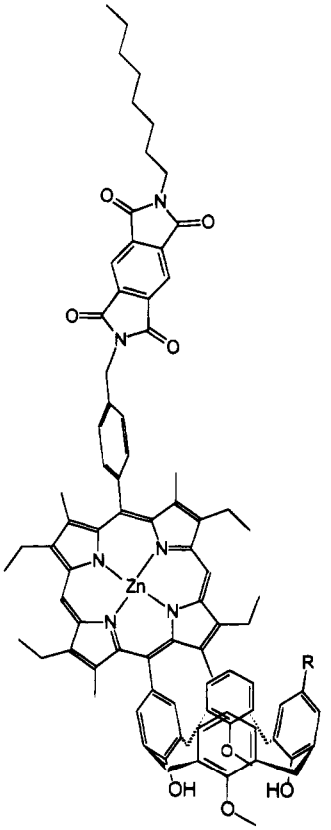

7: $R = NO_2$
8: $R = NH_2$

7 was reduced to the corresponding amine with $SnCl_2$/aqueous HCl/THF, and zinc was inserted into the porphyrin by stirring with methanolic $Zn(OAc)_2$ in $CHCl_3$ to yield **8** (76%). Target molecule **1** was prepared from **8** by Schiff base formation with excess apo-β-8′-carotenal in refluxing toluene (67%). Molecule **7** was used as a reference molecule because it lacks the carotenoid. In addition, **2** was mononitrated using HNO_3 in acetic anhydride/CH_2Cl_2 to give 5-nitrocalix[4]arene, **9** (71%). The nitro group of **9** was reduced to the corresponding amine with $SnCl_2$/aqueous HCl/THF to yield **10** (96%). Carotenoid-only reference **11** was prepared from **10** by reflux of the amine with excess apo-β-8′-carotenal in toluene (63%).

Spectroscopy. The ground state absorption spectra of **1** and **7** shown in Figure 1 are simply the sums of the absorption spectra of the individual chromophores. Transient absorption spectra of molecules **1** and **7** in toluene at 150 ps following excitation with 130 fs, 412 nm laser pulses, Figure 2, show characteristic absorption bands of ZP^+ and PI^- at 660 nm[17] and 720 nm,[18] respectively. Monitoring the kinetics of ZP^+–PI^- ion pair formation and decay at 720 nm, Figure 3, shows that the ion pair is formed in toluene with a 64 ps time constant (97% quantum yield) and decays with a 3.7 ns time constant.

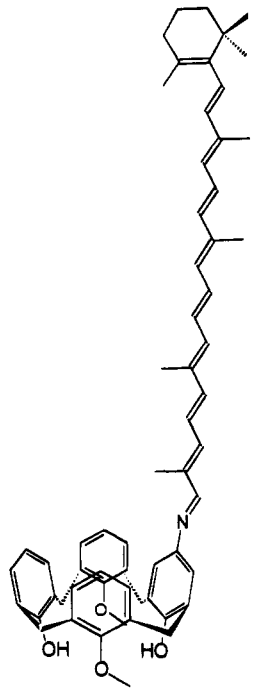

11

It is important to establish that the photophysical properties of the carotenoid observed following excitation of ZP–PI are due to electric field effects alone and not to excited or ionic states of the carotenoid produced after excitation. In **1** the porphyrin absorption at 412 nm is about 8 times larger than that of the carotenoid. Therefore, the carotenoid is excited in a small fraction of the molecules. Excitation of the carotenoid-only reference compound, **11**, at 412 nm results in a sub-picosecond rise time for the carotenoid lowest excited singlet state that decays with a 9.1 ps time constant, Figure 4.[19] To be certain that the entire population of carotenoid molecules is in its ground electronic state, we examine the transient spectra of ZP–PI and the carotenoid in **1** at 150 ps, a time much longer than the decay time of the carotenoid excited state. The formation of ZP^+–PI^- does not result in oxidation or reduction of the adjacent carotenoid because the carotenoid is 150 mV more difficult to oxidize than ZP, while the carotenoid is 800 mV harder to reduce than PI.[14,20] In addition, there is no evidence for the formation of carotenoid ions in the transient spectra.[21]

Changes in the ground state optical absorption spectrum of the carotenoid due to the presence of the electric field produced by ZP^+–PI^- within **1** were determined from the difference spectrum calculated by subtracting the transient absorption spectrum of reference molecule **7** from that of **1** at 150 ps following excitation. The two absorption bands at 660 and 720 nm in the spectra from both molecules in Figure 2 were used as internal standards, because they are well removed from the carotenoid absorption band region, and are due solely to the presence of the charge-separated species, ZP^+–PI^-. By nulling these two bands during subtraction, we correct for any small differences in concentration of ZP^+–PI^- between the two samples. Figure 5 shows the resulting difference spectrum

(16) Osuka, A.; Yamada, H.; Maruyama, K.; Mataga, N.; Asahi, T.; Ohkouchi, M.; Okada, T.; Yamazaki, I.; Nishimura, Y. *J. Am. Chem. Soc.* **1993**, *115*, 9439.

(17) Fajer, J.; Borg, D. C.; Forman, A.; Dolphin, D.; Felton, R. H. *J. Am. Chem. Soc.* **1970**, *92*, 3451.

(18) Osuka, A.; Nakajima, S.; Maruyama, K.; Mataga, N.; Asahi, T. *Chem. Lett.* **1991**, 1003.

(19) Wasielewski, M. R.; Kispert, L. D. *Chem. Phys. Lett.* **1986**, *128*, 238.

(20) Khaled, M.; Hadjipetrou, A.; Kispert, L. D. *J. Phys. Chem.* **1990**, *94*, 5164.

(21) Bensasson, R. V.; Land, E. J.; Truscott, T. G. *Flash Photolysis and Pulse Radiolysis*; Pergamon: Oxford, 1983; p 73.

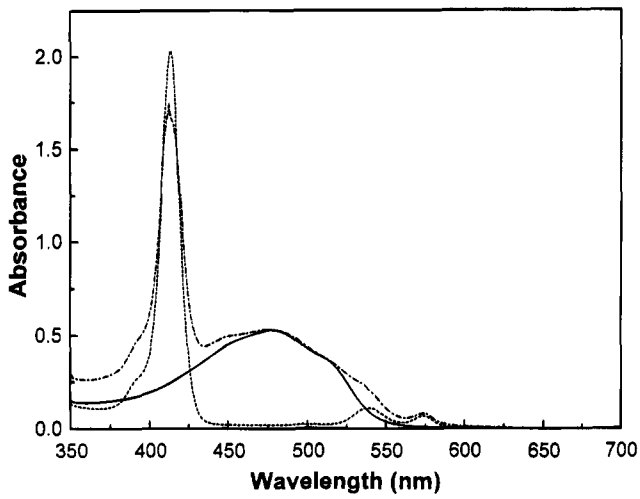

Figure 1. Ground state absorption spectra of **1** (— • — •), **7** (- - -), and **11** (—) in toluene.

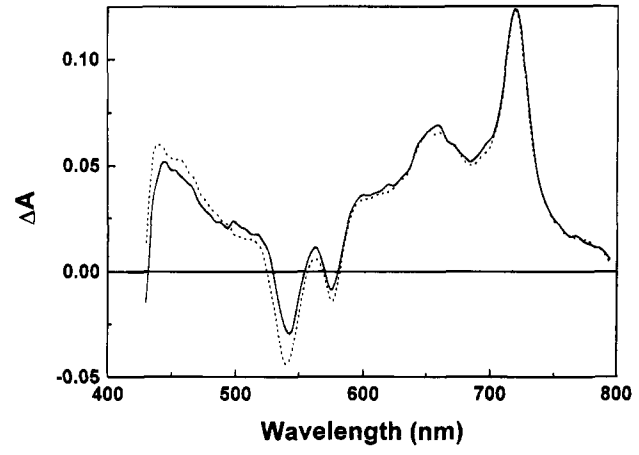

Figure 2. Transient absorption spectra of **7** (- - -) and **1** (—) in toluene 150 ps after excitation with a 412 nm, 5 μJ, 130 fs laser pulse.

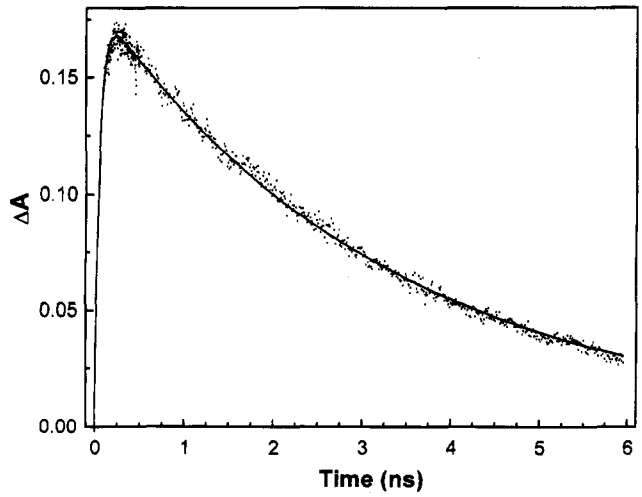

Figure 3. Transient absorption kinetics of **1** (—) in toluene monitored at 720 nm after excitation with a 412 nm, 5 μJ, 130 fs laser pulse.

recorded in toluene (ϵ = 2.4)[22] along with one measured in benzonitrile (ϵ = 25).[22] We assign the derivative-shaped ΔA change observed for **1** in toluene to a 15 nm electrochromic red shift of the carotenoid absorption band. Figure 5 shows that no electrochromic shift is observed in benzonitrile. The 10-fold increase in dielectric constant in going from toluene to

(22) Riddick, J. A.; Bunger, W. B.; Sakano, T. K. In *Organic Solvents*, 4th ed.; Wiley-Interscience: New York, 1986.

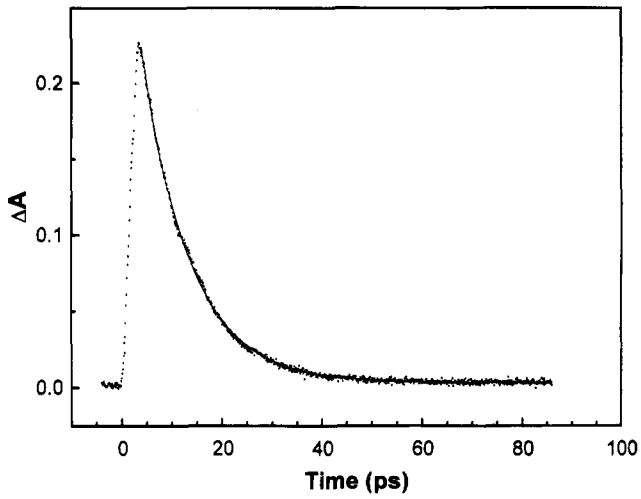

Figure 4. Transient absorption kinetics of **11** (—) in toluene monitored at 560 nm after excitation with a 412 nm, 5 μJ, 130 fs laser pulse.

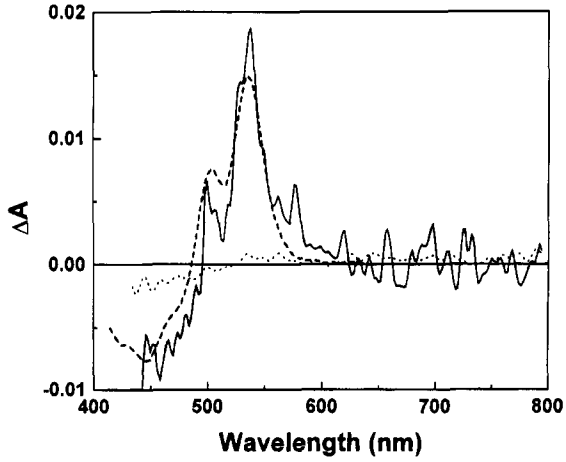

Figure 5. Electrochromically shifted ground state spectra of the carotenoid molecule within **1** at 150 ps following production of ZP^+-PI^- in toluene (—) and benzonitrile (• • •). The simulated 15 nm band shift (- - -) of the carotenoid ground state spectrum is superimposed on the data.

benzonitrile should substantially reduce the electric field strength at the carotenoid. In principle, the transient absorption spectrum of ZP^+-PI^- in benzonitrile could be used as a reference for the electric field effect observed in toluene. However, the 720 nm absorption band of PI^- broadens and diminishes in intensity in solvents having high dielectric constants.[18]

Discussion

In general the intensity, frequency, and bandwidth of an electronic transition can be affected by an electric field. Liptay has discussed these effects for molecules in solution.[23-25] Application of an external electric field to an ensemble of molecules in solution that possess significant ground state dipole moments and/or polarizabilities results in small changes in the average orientation of the molecules relative to the field. When this ensemble is excited with polarized light, electric field dependent changes in the intensity of electronic transitions in the molecules are observed. These changes depend on the scalar product of the vector along which the light is polarized and the transition moment vector. Additional complexities arise if the

(23) Liptay, W. *Angew. Chem., Int. Ed. Engl.* **1969**, *3*, 177.
(24) Liptay, W. *Z. Naturforsch. A* **1965**, *20*, 1441.
(25) Liptay, W. In *Excited States*; Lim, E., Ed.; Academic Press: New York, 1975; Vol. 1, p 129.

ground state and electronic transition polarizabilities are significant. In compound **1** formation of ZP^+-PI^- produces an electric field with an orientation that on average points in a particular direction relative to the molecular axis system of the probe molecule. This direction is dictated primarily by the conformation of the calix[4]arene spacer. Thus, in **1** the electric field itself does not provide the primary method of orienting the sample. This simplifies the analysis of the field effect on the electronic transitions of the probe molecule. Such field dependent orientation effects have recently been used to probe on a sub-nanosecond time scale the dipole moment changes that occur in donor–acceptor complexes.[26]

Electric field dependent changes in the frequency of a transition depend on the difference in dipole moments and polarizability tensors between the ground and excited states of a molecule.[23–25] The dipole moment of a molecule in an electric field **F** is given by

$$\boldsymbol{\mu}^{\mathbf{F}} = \boldsymbol{\mu} + \boldsymbol{\alpha}\cdot\mathbf{F} \tag{1}$$

where $\boldsymbol{\mu}^{\mathbf{F}}$ and $\boldsymbol{\mu}$ are the dipole moment vectors in the presence and the absence of the electric field, **F**, respectively, and $\boldsymbol{\alpha}$ is the polarizability tensor. The interaction energy of the dipole moment $\boldsymbol{\mu}^{\mathbf{F}}$ with the field **F** is

$$E = -\int \boldsymbol{\mu}^{\mathbf{F}}\, \mathrm{d}\mathbf{F} \tag{2}$$

Thus, the corresponding interaction energies of a molecule with an electric field in its ground and excited states are respectively

$$E_g = -\int (\boldsymbol{\mu}_g^{\mathbf{F}}\cdot\mathbf{F})\, \mathrm{d}\mathbf{F} = -\left(\boldsymbol{\mu}_g + \frac{1}{2}\boldsymbol{\alpha}_g\cdot\mathbf{F}\right)\cdot\mathbf{F} \tag{3}$$

$$E_e = -\int (\boldsymbol{\mu}_e^{\mathbf{F}}\cdot\mathbf{F})\, \mathrm{d}\mathbf{F} = -\left(\boldsymbol{\mu}_e + \frac{1}{2}\boldsymbol{\alpha}_e\cdot\mathbf{F}\right)\cdot\mathbf{F} \tag{4}$$

where $\boldsymbol{\mu}_g$ and $\boldsymbol{\mu}_e$ are the ground and excited state dipole moment vectors in the absence of the field **F**, and $\boldsymbol{\alpha}_g$ and $\boldsymbol{\alpha}_e$ are the corresponding polarizability tensors. Thus, the change in frequency of the electronic transition, i.e., the band shift, is given by

$$\Delta\nu = -\frac{1}{h}\left[(\boldsymbol{\mu}_e - \boldsymbol{\mu}_g) + \frac{1}{2}(\boldsymbol{\alpha}_e - \boldsymbol{\alpha}_g)\cdot\mathbf{F}\right]\cdot\mathbf{F} \tag{5}$$

The direction and magnitude of the shift depend on the difference in permanent dipole moment vectors and the difference in polarizability tensors between the ground and excited states, in addition to the magnitudes and orientations of these vector and tensor differences with respect to the electric field vector. An analysis of the data for compound **1** must first consider the average orientation of the ZP^+-PI^- ion pair relative to that of the carotenoid.

The conformation of **1** was calculated using the MM2 force field.[10] The calculated structure places the average distance of the unsaturated carbon atoms of the carotenoid at 8 Å from the midpoint of a line joining the center of ZP^+ to the center of PI^-. Figure 6 shows the geometric relationship between ZP, PI, and the carotenoid in the calculated structure. Connecting atoms have been removed for clarity. The calculated dihedral angle between the two phenols bearing ZP–PI and the carotenoid is 35°. The calix[4]arene in the calculated structure adopts the cone conformation, which agrees well with the proton NMR data obtained on **1**. The CH_2 protons that bridge the phenol rings in the calix[4]arene spacer appear as an AB quartet at δ = 4.45 and 4.65 ppm with a geminal coupling constant J = 13 Hz. These values are typical of the cone formation in the calix[4]arene.[12,13]

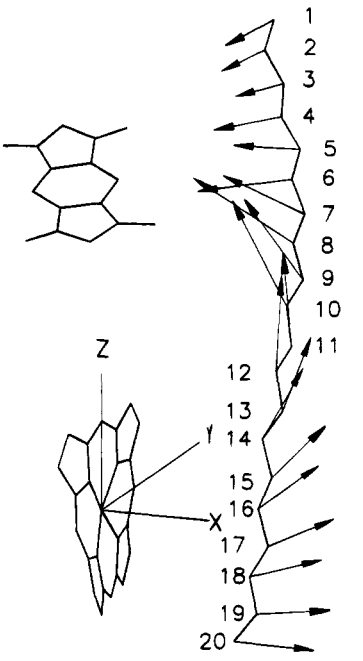

Figure 6. Structure of **1** calculated using the MM2 force field. Only the atoms in the π systems of the porphyrin and pyromellitimide are shown, in addition to the unsaturated carbon atoms in the C–C backbone of the carotenoid. The numbers of the atoms correspond to those given in Table 1. The arrows attached to the carotenoid atoms are scaled to the direction and magnitude of the calculated electric field at these atoms.

The diamagnetic ring current of the porphyrin can be used to verify whether the distance between the porphyrin and the carotenoid predicted by the calculated structure is reasonable. Proton NMR data on **1** shows that the ring current of the porphyrin shifts the resonance of the proton attached to the carotenoid Schiff base carbon atom downfield by 0.26 ppm, while the protons of the methyl group on the second carbon down the carotenoid backbone from the Schiff base nitrogen atom are shifted by 0.16 ppm upfield. Using the model given by Abraham for predicting the chemical shifts of paramagnetic nuclei close to porphyrins,[27] the distance of these protons from the Zn atom at the center of the porphyrin macrocycle are 8.2 and 7.8 Å, respectively. These values are consistent with the respective 7.5 and 7.0 Å distances for these protons predicted by the force field calculation. Carotenoid protons further away from the Schiff base nitrogen atom are not shifted significantly by the porphyrin ring current. The 35° dihedral angle between the phenols bearing the field generator and carotenoid results in larger distances between these two components as one moves toward the cyclohexene ring of the carotenoid. The proton NMR data suggests that the structure of **1** obtained from the force field calculation is a reasonable point of departure for analyzing the influence of the ZP^+-PI^- electric field on the carotenoid.

Molecular orbital calculations on a variety of carotenoids using the AM1 method with CI clearly indicate that the dipole moments in both the ground and excited states of these polyenes are approximately collinear and lie along the C–C backbone of the molecule.[28] Thus, the first term in eq 5 reduces to

(26) Smirnov, S. N.; Braun, C. L. *J. Phys. Chem.* **1994**, *98*, 1953.

(27) Abraham, R.; Bedford, G. R.; McNeillie, D.; Wright, B. *Org. Magn. Reson.* **1980**, *14*, 418.

(28) O'Neil, M. P.; Wasielewski, M. R.; Khaled, M. M.; Kispert, L. D. *J. Chem. Phys.* **1991**, *95*, 7212.

$$(\boldsymbol{\mu}_e - \boldsymbol{\mu}_g)\cdot\mathbf{F} = (\mu_e - \mu_g)F\cos\theta \quad (6)$$

where θ is the angle between electric field direction and the direction of $(\boldsymbol{\mu}_e - \boldsymbol{\mu}_g)$. As a consequence of the fact that the difference dipole moment is oriented along the carotenoid C−C backbone, θ is also the direction of the field vector relative to a vector along the carotenoid C−C backbone. On average, the field generated by the ZP^+-PI^- ion pair points along a line from the center of the ZP macrocycle to the center of the benzene ring of the pyromellitimide acceptor. The negative end of the difference dipole moment vector on the polyene points along the C−C backbone toward the Schiff base nitrogen atom. Thus, if we neglect for now the polarizability term in eq 5, eqs 5 and 6 predict that, for angles $-90° < \theta < 90°$, the field effect on the probe molecule will shift the optical transition to lower frequency.

An electrostatic calculation was performed on **1** to more quantitatively assess the magnitude and direction of the electric field produced by the charge distribution within the ZP^+-PI^- ion pair at each unsaturated carbon atom of the adjacent carotenoid. The charge distributions within ZP^+ and PI^- were calculated using the AM1 molecular orbital treatment. The geometry of **1** was assumed to be that calculated by MM2 and shown in Figure 6. The electric fields resulting from the distributed charges at each atomic position within ZP^+ and PI^- were summed vectorially at each unsaturated carbon atom of the carotenoid backbone. These values are listed in Table 1. The electric field strengths vary from 8.7 to 22.8 MV/cm. The average electric field at the carotenoid was determined by summing the electric field vector components at each unsaturated carbon atom along the carotenoid and then dividing each component by the number of atoms in the chain. The magnitude of this average field vector is 10.0 MV/cm. The use of this average field vector to gauge the degree of interaction of the field with the difference dipole moment vector and difference in polarizability tensors between the ground and excited states of the carotenoid depends on the assumption that each atom in the carotenoid backbone contributes equally to these quantities. In general, this is not rigorously correct and therefore represents an approximation. Further, if we assume that the solvent surrounding **1** can be described by the continuum model, the average calculated electric field at the carotenoid in toluene (ϵ = 2.4) is 10.0/2.4 = 4.2 MV/cm. Given the close distance between the ZP−PI field generator and the carotenoid probe, use of the bulk dielectric constant is suspect. However, the use of a more detailed electrostatic model for the solvent is unwarranted at this time due to the absence of structural information regarding the locations and orientations of the toluene molecules surrounding **1**.

The tensorial nature of $\boldsymbol{\alpha}_e$ and $\boldsymbol{\alpha}_g$ complicates the analysis of the second term in eq 5. However, the dominant components of both $\boldsymbol{\alpha}_e$ and $\boldsymbol{\alpha}_g$ most likely lie along the C−C backbone of carotenoid, the probe molecule.[29,30] Because the difference dipole moment between the ground and excited states of the carotenoid is relatively small, an estimate of the change in polarizability due to excitation must be included. Thus,

$$\frac{1}{2}[(\boldsymbol{\alpha}_e - \boldsymbol{\alpha}_g)\cdot\mathbf{F}]\cdot\mathbf{F} = \frac{1}{2}(\alpha_e^{zz} - \alpha_g^{zz})F^2\cos^2\phi \quad (7)$$

where ϕ is the angle between the electric field vector and the principal (zz) component of the polarizability of the carotenoid. In the case of long chain polyenes the variables θ and ϕ in eqs 6 and 7, respectively, are approximately the same. The use of these assumptions certainly results in an oversimplified description of the complex interactions between the difference dipole moments, tensors, and the field. Nevertheless, we can test whether the experimental results can be described adequately using this simplified treatment.

Table 1. Calculated Electric Field Produced by ZP^+-PI^- at Each Unsaturated Carbon Atom in the Backbone of the Carotenoid in **1**

atom no.	field magnitude (MV/cm)	field vector components (MV/cm)		
		x	y	z
1	8.65	−2.867	−8.064	−1.249
2	11.25	−4.279	−10.242	−1.824
3	11.68	−5.175	−10.472	−0.299
4	14.87	−7.856	−12.624	−0.041
5	14.60	−8.097	−11.796	2.892
6	19.24	−12.445	−13.946	4.563
7	18.28	−10.890	−11.609	8.983
8	22.77	−14.493	−11.349	13.406
9	19.27	−8.301	−7.387	15.743
10	21.94	−8.094	−5.365	19.675
11	17.99	−0.630	−2.959	17.738
12	18.34	1.558	−1.791	18.182
13	15.71	5.845	−1.246	14.528
14	16.31	8.173	−1.298	14.057
15	14.90	10.223	−0.997	10.791
16	15.06	11.684	−1.321	9.416
17	14.11	12.514	−1.089	6.429
18	14.86	13.934	−1.574	4.930
19	14.41	14.095	−1.628	2.494
20	16.10	15.850	−2.772	0.683

The electrochromic red shift in **1** was simulated by recording the ground state spectrum of **11**, calculating a spectrum shifted by -630 cm^{-1}, and taking the difference between these two spectra (Figure 5). The fidelity of the simulation in Figure 5 to the data suggests that the observed electrochromism is dominated by the band shift contribution. If the presence of the electric field resulted in a strong intensity change in the carotenoid $S_0 \leftarrow S_2$ transition, a simple band shift model would not adequately describe the data. Electric field dependent intensity changes of an electronic transition involve the interaction of the field with the transition moment and polarizability of the transition. Our data suggests that these changes are not significant in **1**. The wavelength shift must therefore come from the interaction of **F** with $\Delta\boldsymbol{\mu}$ and $\Delta\boldsymbol{\alpha}$. In asymmetric polyenes the magnitude of $\Delta\boldsymbol{\mu}$ is about $2-4 \times 10^{-29}$ C m (6−12 D),[28-31] while very large values of the magnitude of $\Delta\boldsymbol{\alpha}$ on the order of 10^{-37} C V^{-1} m^2 have been reported.[29,30] Unfortunately, the accuracy of the $\Delta\boldsymbol{\alpha}$ values is low. However, using eqs 5−7, with $\theta = \phi = 35°$, $\Delta\boldsymbol{\mu} = 2 \times 10^{-29}$ C m, and $\Delta\boldsymbol{\alpha} = 10^{-37}$ C V^{-1} m^2, along with $\Delta\nu = -630$ cm^{-1}, eq 5 yields $F = 5.5$ MV/cm at the carotenoid.

The experimental data along with eqs 5−7 yields the average value of the electric field at the carotenoid in solution. This number can be compared with the value of F obtained from the electrostatic calculation given above. Assuming a dielectric constant of 2.4 for toluene, we calculated $F = 4.2$ MV/cm. The agreement between the experimentally determined 5.5 MV/cm field value and that obtained from the electrostatic calculation is reasonably good. Given our incomplete knowledge of the directions and magnitudes of the polarizability tensors in the ground and excited states of the carotenoids and the appropriate way in which to model the solvent in the vicinity of the field generator and probe molecules, one should view this agreement cautiously.

Given these caveats, the data suggests that the dielectric continuum model of the solvent remains a surprisingly good

(29) Labhart, H. In *Advances in Chemical Physics*; Prigogine, I., Ed.; Wiley-Interscience: New York, 1967; Vol. 13, p 179.
(30) Ponder, M.; Mathies, R. *J. Phys. Chem.* **1983**, *87*, 5090.
(31) Mathies, R.; Stryer, L. *Proc. Natl. Acad. Sci. U.S.A.* **1976**, *73*, 2169.

approximation in this experiment. We have noted previously that, under certain circumstances, the continuum model of the solvent is reasonably robust. For example, the continuum model yields reasonable values of ion pair solvation energies in covalently-linked porphyrin−quinone molecules in which the sizes of the ions and the close distance between them within the photochemically generated ion pair would lead us to be skeptical.[32] Exploration of other systems with better defined geometries and, perhaps, even restrictions on solvent motion may be required to validate the use of particular solvation models in this treatment. In fact, careful studies of the dependence of the observed electric field effect in systems such as **1** on solvent dielectric properties could prove useful in probing solvent structure around the field generator and probe molecules.

Conclusions

The 5.5 MV/cm electric field strength produced by the ZP^+-PI^- ion pair at the adjacent carotenoid probe molecule is larger than fields that can be produced conveniently from external, pulsed high voltage sources before dielectric breakdown of the thin film samples occurs. This electric field shifts the absorption band of the carotenoid 80 meV lower in energy. This raises the possibility that such an intense, localized electric field could be used to perturb electron transfer in a nearby, isolated donor−acceptor system by, in effect, tuning its redox potential and thereby modifying its electron transfer rate constants. We are exploring this possibility.

Experimental Section

Proton NMR spectra were obtained on a Bruker AM-300 300 MHz spectrometer. Mass spectra were obtained with a Kratos MALDI spectrometer. UV−vis spectra were obtained with a Shimadzu UV-160 spectrometer. Merck silica gel 60 was used for column chromatography. All solvents were reagent grade.

Synthesis. 25,27-Dihydroxy-26,28-dimethoxy-5-formylcalix[4]arene (3). 25,27-Dihydroxy-26,28-dimethoxycalix[4]arene (**2**) (1.45 g, 3 mmol) was dissolved in CH_2Cl_2 (120 mL), and the solution was cooled to 0 °C under a nitrogen atmosphere. Dichloromethyl methyl ether (1.2 equiv, 0.33 mL) was added, and the solution was stirred for 10 min. Titanium tetrachloride (1.5 mL) was added, and stirring was continued for 1 h. Water (300 mL) was added, followed by stirring for 30 min. The organic layer was washed with aqueous sodium bicarbonate (300 mL × 2) and water (300 mL) and dried over anhydrous sodium sulfate, and the solvent was evaporated. The purification by silica gel column chromatography (2% acetone in CH_2Cl_2) gave **3** in 82% yield (1.57 g, 2.5 mmol): mp 254−256 °C; ^{1}H-NMR ($CDCl_3$) 9.81 (s, 1H, CHO), 8.72 (s, 1H, OH), 7.74 (s, 1H, OH), 7.65 (s, 2H, Ar), 7.09 (d, 2H, J = 7.5 Hz, Ar), 6.87 (d + d, 4H, Ar), 6.75 (d + d + d, 3H, Ar), 4.30 (d + d, 4H, CH_2), 4.01 (s, 6H, Me), 3.7 (d + d, 4H, CH_2); mass spectrum *m/e* calcd 480.3, found (M^+ + 23) 503.3.

25,27-Dihydroxy-26,28-dimethoxy-5-formyl-17-nitrocalix[4]arene (4). Calixarene **3** (480 mg, 1 mmol) was dissolved in CH_2Cl_2 (50 mL), and 0.5 mL of acetic acid was added under a nitrogen atmosphere. After an addition of 1.12 equiv of 70% nitric acid (72 μL) the mixture was stirred for 2.5 h. Water (50 mL) was added, and the organic layer was washed with aqueous sodium bicarbonate (50 mL × 2) and water (50 mL × 2) and then dried over anhydrous sodium sulfate. After the solvent was removed, the residue was rinsed with cold THF, and the pure **4** was obtained in 62% yield (327 mg, 0.62 mmol): mp >300 °C, ^{1}H-NMR ($CDCl_3$) 9.82 (s, 1H, CHO), 8.99 (s, 1H, OH), 8.74 (s, 1H, OH), 8.06 (s, 2H, Ar), 7.66 (s, 2H, Ar), 6.92 (d of d, 4H, Ar), 6.81 (d of d, 2H, Ar), 4.30 (d, 4H, J = 13.3 Hz, CH_2), 4.03 (s, 6H, Me), 3.57 (d of d, 4H, CH_2); mass spectrum *m/e* calcd 525.3, found 525.2.

(32) Gaines, G. L., III; O'Neil, M. P.; Svec, W. A.; Niemczyk, M. P.; Wasielewski, M. R. *J. Am. Chem. Soc.* **1991**, *113*, 719.

Porphyrin−Calix[4]arene (7). To the solution of calixarene **4** (105 mg, 0.2 mmol) and *N*-((4-formylphenyl)methyl)-*N'*-octyl-1,2:4,5-benzenebis(dicarboximide) (**5**) (178 mg, 0.4 mmol) in CH_2Cl_2/CH_3CN (22−30 mL) was added 3,3'-dimethyl-4,4'-diethyldipyrrylmethane (**6**) (138 mg, 0.6 mmol) under a nitrogen atmosphere. After the addition of trichloroacetic acid (30 mg, 0.18 mmol) in 3 mL of CH_3CN, the mixture was stirred for 19 h in the dark. Chloranil (300 mg, 1.22 mmol) in 15 mL of CH_2cl_2 was added, and the stirring was continued for 2.5 h. The mixture was diluted with 50 mL of CH_2Cl_2, washed with aqueous sodium bicarbonate (100 mL × 3) and water (100 mL × 2), and dried over anhydrous sodium sulfate. After the solvent was removed, the residue was dissolved in 50 mL of CH_2Cl_2 and 0.5 mL of saturated zinc acetate in methanol was added. After stirring for 30 min, the solvent was removed and the residue was rinsed with methanol. The cross-condensation product was separated on silica gel column chromatography (0.1−0.5% acetone in CH_2Cl_2). Crystallization from $CH_2Cl_2CH_3OH$ gave **7** in 22% yield (62 mg, 44 μmol): mp 238−240 °C (dec); ^{1}H-NMR ($CDCl_3$) calixarene 9.11 (s, 1H, OH), 8.36 (s, 1H, OH), 8.03 (s, 2H, Ar), 7.80 (s, 2H, Ar), 7.07 (dd, 2H, Ar), 6.98 (d, 2H, Ar), 6.88 (d, 2H, Ar), 4.60 (d, 2H, CH_2), 4.40 (d, 2H, CH_2), 4.12 (s, 6H, OMe), 3.5−3.8 (d of d, 4H, CH_2), porphyrin 10.18 (s, 1H, meso), 10.16 (s, 1H, meso), 8.03 (d, 2H, J = 7.8 Hz, Ar), 7.75 (d, 2H, J = 7.8 Hz, Ar), 4.0 (m, 8H, CH_2CH_3), 2.63 (s, 3H, Me), 2.39 (s, 6H, Me), 1.98 (s, 3H, Me), 1.75 (m, 12H, CH_2CH_3), imide 8.19 (s, 2H, Ar), 5.26 (s, 2H, benzylic), 3.75 (t, 2H, octyl-1), 1.75 (m, 2H, octyl-2), 1.3 (m, 10H, octyl-3,4,5,6,7), 0.88 (t, 3H, octyl-8); mass spectrum *m/e* calcd 1453.3, found 1453.7.

Porphyrin−Calix[4]arene (8). Porphyrin **7** (104 mg, 71 μmol) was dissolved in distilled THF (50 mL), tin(II) chloride dihydrate (4.4 mmol, 1 g) in 3 mL of concentrated HCl was added, and the stirring was continued for 24 h. During the stirring, tin(II) chloride hydrate (4.4 mmol, 1 g) in concentrated HCl (3 mL) was added three times. Then 100 mL of $CHCl_3$ was added, and the organic layer was washed with aqueous potassium hydroxide (50 mL × 2) and water (50 mL) and dried over anhydrous sodium sulfate. The solvent was evaporated, and the residue was converted to zinc compounds as described above for porphyrin **7**. Purification by silica gel column chromatography (3% acetone in CH_2Cl_2) and crystallization from $CH_2Cl_2CH_3OH$ gave **8** in 37% yield (37 mg, 26 μmol): mp 245−247 °C (dec); ^{1}H-NMR ($CDCl_3$) calixarene 8.04 (s, 1H, OH), 7.90 (s, 1H, OH), 7.78 (s, 2H, Ar), 7.01 (d, 2H, Ar), 6.9 (d + d, 4H, Ar), 6.12 (s, 2H, Ar), 4.60 (d, 2H, J = 13.1 Hz, CH_2), 4.34 (d, 2H, J = 13.1 Hz, CH_2), 4.07 (s, 6H, OMe), 3.6 (d, 2H, CH_2), 3.28 (d, 2H, J = 13.0 Hz, CH_2), porphyrin 10.17 (s, 1H, meso), 10.14 (s, 1H, meso), 8.04 (d, 2H, Ar), 7.78 (d, 2H, Ar), 4.0 (m, 8H, CH_2CH_3), 2.61 (s, 3H, Me), 2.42 (s, 6H, Me), 1.98 (s, 3H, Me), 1.74 (m, 12H, CH_2CH_3), imide 8.32 (s, 2H, Ar), 5.26 (s, 2H, benzylic), 3.7 (m, 2H, octyl-1), 1.74 (m, 2H, octyl-2), 1.3 (m, 10H, octyl-3,4,5,6,7), 0.99 (t, 3H, octyl-8); mass spectrum *m/e* calcd 1425.3, found 1425.5.

Porphyrin−Calix[4]arene−Carotene (1). Porphyrin **8** (35 mg, 25 μmol) was dissolved in toluene (15 mL), and 8'-*apo*-β-carotenal (41 mg, 0.1 mmol) was added. The solution was refluxed under a nitrogen atmosphere in the dark for 48 h. After cooling, the mixture was poured onto silica gel and separated with 2% acetone in CH_2Cl_2 to yield 67% of **1** (30 mg, 17 μmol): mp 178−180 °C (dec); ^{1}H-NMR ($CDCl_3$) 10.19 (s, 1H, meso), 10.16 (s, 1H, meso), 8.36 (s, 2H, Im-Ar), 8.26 (s, 1H, OH), 8.06 (d, 2H, Ar), 7.94 (s, 1H, OH), 7.88 (s, 1H, N = CH), 7.79 (d, 2H, J = 8.0 Hz, Ar), 7.75 (d, 2H, J = 8.0 Hz, Ar), 7.13 (s, 2H, calix-Ar), 7.04 (d of d, 4H, calix-Ar), 6.1−7.0 (m, 14H, polyene, calix-Ar), 5.30 (s, 2H, benzylic), 4.65 (d, 2H, J = 13.2 Hz, calix-CH_2), 4.45 (d, 2H, J = 13.2 Hz, calix-CH_2), 4.11 (s, 6H, Me), 4.0 (m, 8H, CH_2CH_3), 3.8 (t, 2H, octyl-1), 3.6 (d of d, 4H, calix-CH_2), 2.63 (s, 3H, Me), 2.40 (s, 6H, Me), 2.23 (s, 3H, Me), 2.0 (14H, 4 s and 1 m, 4Me, CH_2), 1.7 (m, 19H, $4CH_2CH_3$ and CH_2 and Me and octyl-2), 1.5 (m, 2H, CH_2), 1.3 (m, 10H, octyl-3,4,5,6,7), 1.05 (s, 6H, 2Me), 0.91 (m, 3H, octyl-8); mass spectrum *m/e* calcd 1824.6, found 1824.3.

25,27-Dihydroxy-26,28-dimethoxy-5-nitrocalix[4]arene (9). 25,27-Dihydroxy-26,28-dimethoxycalix[4]arene (**2**) (2 mmol, 914 mg) was dissolved in CH_2Cl_2 (100 mL) and acetic acid (1 mL), and 70% nitric acid (2.24 mmol, 288 μL) was added. The mixture was stirred at room temperature for 1 h under a nitrogen atmosphere. The mixture was diluted with $CHCl_3$ (100 mL), washed with aqueous sodium bicarbonate

(100 mL × 2) and water (100 mL × 2), and dried over anhydrous sodium sulfate. The solvent was evaporated, and the residue was purified by silica gel column chromatography (CH_2Cl_2), to obtain **9** in 71% yield (705 mg, 1.4 mmol): mp >300 °C. ^{1}H-NMR ($CDCl_3$) 8.95 (s, 1H, OH), 8.07 (s, 1H, OH), 8.07 (s, 2H, Ar), 7.78 (s, 2H, Ar), 6.92 (m, 4H, Ar), 6.81 (m, 2H, Ar), 4.30 (d, 2H, J = 13.2 Hz, CH_2), 4.28 (d, 2H, J = 13.2 Hz, CH_2), 4.04 (s, 6H, OMe), 3.54 (d, 4H, J = 13.2 Hz, CH_2); mass spectrum *m/e* calcd 497.3, found 496.8.

5-Amino-25,27-dihydroxy-26,28-dimethoxycalix[4]arene (10). To a solution of **9** (1 mmol, 497 mg) in absolute ethanol (50 mL) was added 1 g of 10% palladium on carbon under a nitrogen atmosphere. The solution was heated to reflux, and 12.5 mL of hydrazine monohydrate was added dropwise. The color of the solution changed to yellow. After 30 min, the solution became colorless again. After 30 min of additional reflux, the solution was poured into $CHCl_3$ (300 mL). After cooling to room temperature, palladium on carbon was filtered off. The solution was washed with water (200 mL × 3) and dried over anhydrous sodium sulfate. After the solvent was removed, the residue was crystallized from benzene and **10** was obtained in 96% yield (0.96 mmol, 448 mg): mp 284−286 °C (dec); ^{1}H-NMR (DMSO-d_6) 7.70 (s, 1H, OH), 7.12 (s, 1H, OH), 7.07 (d, 2H, 7.5 Hz, Ar), 6.86 (m, 4H, Ar), 6.70 (m, 3H, Ar), 6.48 (s, 2H, Ar), 4.30 (d, 2H, J = 13.2 Hz, CH_2), 4.28 (d, 2H, J = 13.2 Hz, CH_2), 3.96 (s, 6H, OMe), 3.50 (d, 4H, J = 13.2 Hz, CH_2), 3.42 (d, 2H, J = 13.2 Hz, CH_2); mass spectrum *m/e* calcd 467.3, found 466.9.

Calix[4]arene−Carotene (11). Aminocalixarene **10** (24 mg, 0.05 mmol) was dissolved in 15 mL of toluene, and 8′-apo-β-carotenal (41 mg, 0.1 mmol) was added. The solution was heated to reflux under a nitrogen atmosphere in the dark. After refluxing for 24 h, the solution was cooled to room temperature, and the solvent was evaporated on a rotary evaporator. Column chromatography of the reaction mixture on silica gel eluting with 3% acetone in $CHCl_3$ gave a 63% yield of **11**: mp 165−167 °C (dec); ^{1}H-NMR ($CDCl_3$) calixarene 7.70 (s, 1H, OH), 7.12 (s, 1H, OH), 7.07 (d, 2H, 7.5 Hz, Ar), 6.86 (m, 4H, Ar), 6.70 (m, 3H, Ar), 6.48 (s, 2H, Ar), 4.30 (d, 2H, J = 14 Hz, CH_2, 4.27 (d, 2H, J = 14 Hz, CH_2), 3.96 (s, 6H, OMe), 3.40 (d, 4H, J =14 Hz, CH_2), 3.28 (d, 2H, J = 14 Hz, CH_2), carotenoid 7.62 (s, 1H, N=*CH*), 6.6−6.9 (m, 5H, polyene), 6.1−6.4 (m, 7H, polyene), 2.16 (s, 3H, Me), 2.0 (m, 11H, CH_2 and 3Me), 1.72 (s, 3H, Me), 1.6 (m, 2H, CH_2), 1.5 (m, 2H, CH_2), 1.03 (s, 6H, 2Me); mass spectrum *m/e* calcd 866.6, found 866.1.

Spectroscopy. Solvents for all spectroscopic experiments were dried and stored over 3 Å molecular sieves. The samples were dissolved in toluene contained in 1 cm path length cuvettes. Following deaeration of the samples by bubbling with nitrogen gas, the cuvettes were sealed. The measurements were carried out on samples with an absorbance of 0.3 at 412 nm in a 1 cm cuvette.

The femtosecond transient absorption apparatus consists of a homemade, self-mode-locked, Ti-sapphire oscillator that is pumped by 6 W, all-lines output from an Ar^+ laser (Laser Ionics 1400). The Ti-sapphire oscillator emits 80 fs, 824 nm pulses at an 81.3 MHz repetition rate with an average power of 400 mW. The 80 fs pulses from the oscillator are temporally stretched using a double-passed grating/mirror combination to a duration of 200 ps. These chirped pulses are amplified with a homemade Ti-sapphire regenerative amplifier that employs a folded cavity and uses a double-step Pockels cell (Medox)/thin film polarizer combination for injection and cavity dumping. The regenerative amplifier is pumped by an intracavity frequency-doubled, Q-switched, Nd:YAG laser (based on a Spectra-Physics 3460 head and a power supply with an Intraaction Q-switch) that produces 3.8 mJ, 250 ns, 532 nm pulses at a 1.27 kHz repetition rate. The output of the Ti-sapphire regenerative amplifier is recompressed with 70% efficiency using a grating pair (ISA) to give 350 μJ, 130 fs, 824 nm pulses at a 1.27 kHz repetition rate. Using appropriate beam splitters about 10 μJ of 824 nm light is used to generate a very smooth white light continuum by focusing it with a 15 cm lens into a 0.5 cm thick block of fused silica. The block is rotated at 1 revolution per day to prevent damage. Frequency chirp in the white light is removed by double-passing the beam off a 300 line/mm grating pair. Shot-to-shot intensity fluctuations of the probe beam are generally less than 5%. The remaining 824 nm light is frequency-doubled with 35% efficiency using a 2 mm long LBO crystal to yield 130 fs, 412 nm pulses.

The energy of the blue excitation light on the sample was varied using a polarizer−λ/2 waveplate combination. Typically, 2−5 μJ was used to excite the molecules. The excitation beam was chopped at 635 Hz synchronized to the laser repetition rate. The white-light probe beam was split into measuring and reference beams. The arrival of the measuring probe beam relative to the excitation beam was accomplished with an optical delay line that used a linear stepping motor (Compumotor) with 1 μm resolution. The nearly-collinear and codirectional excitation and measuring probe beams were focused into the sample to a 0.3 mm diameter. The sample was contained in 1 cm path length cuvette and was stirred. The wavelength of the measuring and reference probe beams were selected with a SPEX M270 monochromator. Changes in the transmission of the measuring probe light through the sample and changes in the reference probe beam were monitored by photodiodes. The output of each photodiode was integrated by a gated integrator (Evans), and both signals were digitized and recorded by a personal computer (Gateway 33 MHz, 486). The data acquisition software monitored the quality of each shot and only averaged shots within 10% of the average intensity of the reference probe beam level. Kinetic parameters were obtained by iterative reconvolution using the Levenberg−Marquardt algorithm. The instrumental time response was 180 fs as determined by cross correlation of the pump and probe beams. Transient absorption spectra at a particular time were obtained by allowing the computer to repetitively scan the monochromator at a fixed delay time between the pump and measuring probe beams. Typically, 20 wavelength scans were averaged.

Acknowledgment. This work was supported by the Division of Chemical Sciences, Office of Basic Energy Sciences of the United States Department of Energy under Contract W-31-109-Eng-38.

JA941336+